

Description of the Liquid-Crystalline Phase of Rodlike Polymers at High Shear Rates

G. Marrucci* and P. L. Maffettone

Università di Napoli, Dipartimento di Ingegneria Chimica, Piazzale Tecchio, 80125 Naples, Italy. Received December 27, 1988; Revised Manuscript Received February 24, 1989

ABSTRACT: The highly nonlinear behavior of the nematic phase of rodlike polymers in shear flow is analyzed by reducing the problem to its two-dimensional analogue. Explicit solutions for the orientational distribution function are found for those situations where a stationary solution in fact exists, i.e., for the nontumbling case. The corresponding stresses are also calculated. It is found that, in a range of shear rates, the normal stress difference is negative. More generally, a very good qualitative agreement is found between theory and experiment.

Introduction

It has long been known that rodlike polymers in concentrated solutions form a liquid-crystalline, nematic phase.^{1,2} It is also well-known by now that the rheology of such a phase is much more complex than that of ordinary polymeric liquids, showing such unusual effects as, e.g., negative normal stresses in a steady shear flow.³⁻⁶

The only available theory describing the rheology of rodlike polymers in the nematic phase is that of Doi,⁷ which, though successful in many respects, does not predict the possible occurrence of negative normal stresses in shear flow. It should be noted, however, that Doi's theory makes use of a mathematical approximation that is not irrelevant. Suffice it to mention that, with the same approximation, the Leslie coefficients which are predicted from the theory⁸ correspond to a stable shear flow with an aligned director, whereas calculations made without that approximation, which are possible in the linear limit,^{9,10} predict tumbling of the director due to shear. Thus, another question that remains open is whether shear flow is or is not of the tumbling type in the nonlinear range.

In this paper, we perform an analysis of the rodlike polymer problem, which provides useful indications for the nonlinear behavior in shear. The trick which makes it possible to proceed with the calculations is doing the analysis in two dimensions instead of three. We are aware, of course, that a change of dimensionality is not exempt of risks. On the other hand, we can thus easily avoid the approximation used by Doi, thereby exploring new possibilities. In the worst case, we will get inspirations on how to tackle the corresponding three-dimensional situation. The two-dimensional analysis proves to be, in fact, extremely rich in results, including the prediction of negative normal stresses in a range of shear rates.

We first present here an intuitive interpretation of the negative normal stress phenomenon, which applies equally well to two or three dimensions and which in fact preceded and motivated the analysis itself. In the following sections, the analysis is developed in necessary detail. The essential results are obtained in closed form, the use of the computer being limited to the calculation of average quantities, i.e., to integrations over a known distribution function.

Explanation of the Negative Normal Stress Phenomenon

The intuitive explanation of the ordinary phenomenon of normal stresses in the shear flow of a polymeric liquid, i.e., when those stresses are positive, is as follows. The isotropic phase of a polymer, be it a flexible polymer or a rigid rodlike one, is characterized by the obvious fact that the distribution of any vectorial quantity associated with the polymeric structure is spherically symmetric at equilibrium. Thus, the end-to-end vector of a flexible chain,

for example, or the unit vector specifying the orientation of a rod is distributed spherically at equilibrium (or "circularly", in two dimensions; see Figure 1).

Shear flow will distort the distribution, making it "ellipsoidal", i.e., of the form schematically depicted in Figure 1. Elastic normal stresses can be associated to such a distribution, which are invariably of the positive type. Indeed, the tendency of the distorted distribution to relax back to the spherical shape implies a traction in the shear direction or, equivalently, a compression orthogonal to it.

Consider now a nematic phase of rodlike polymers. The distribution of the unit vectors specifying rod orientations is already nonspherical at equilibrium. It is elongated in a direction (which is arbitrary at equilibrium) defining the so-called director of the nematic. The spread of rod orientations about the director is usually accounted for by a single scalar quantity, S , called the order parameter, a larger value of S implying a smaller spread. Shear flow will now give rise to two separate effects. On the one hand, there will be an effect on the director. We know already that either the director is made to tumble or it is aligned to some small angle α above the shear direction (see Figure 2). As a second effect, the shear can alter the spread of rod orientations about the director. Now, S can either increase with respect to equilibrium, i.e., the orientational distribution is sharpened by the flow, or decrease, i.e., the ellipsoid becomes blunter.

With reference to Figure 2, assume now that the flow has oriented the director, as well as having created a distribution less peaked than that at equilibrium. There is no doubt that the elastic normal stresses associated with such a situation are negative. Indeed, the relaxation to equilibrium implies an expansion in the shear direction and a contraction orthogonally to it, i.e., the opposite situation to that prevailing in Figure 1.

The plausibility that the flow can in fact generate a larger spread of rod orientations than that existing at equilibrium remains to be examined. In this regard, we recall that shear flow exerts a torque on each rod which, by itself, would make the rod rotate clockwise (in the situation of Figure 2). Thus, rods that are oriented "above" the director (see Figure 3) are pushed toward it, whereas rods sitting "below" the director are pulled away from it. In turn, the nematic potential opposes these tendencies, attempting to reestablish the equilibrium distribution. At steady state, a balance will be struck between the opposing effects, giving rise to some suitably "distorted" distribution. Notice now that, for the rods above the director, the influence of the flow is that of sharpening the distribution. Conversely, for those below, the tendency is that of increasing the spread. Which of these two opposite effects will prevail in a given case cannot be anticipated. There is no reason, however, to exclude a priori any one of the

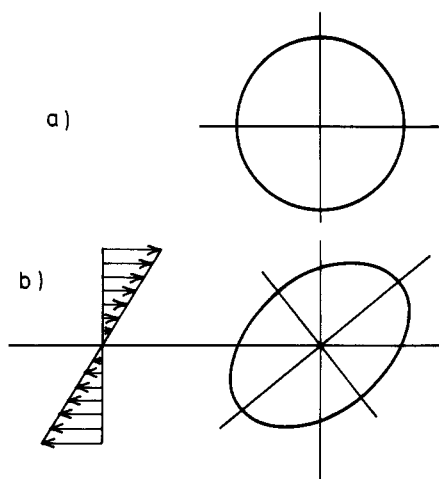


Figure 1. Isotropic phase. The well-known orientational effect of a shear flow. (a) Polar diagram of the orientational distribution at equilibrium. (b) The same diagram under shear.

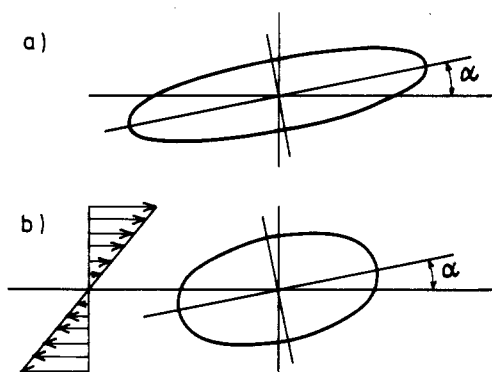


Figure 2. Nematic phase. (a) The equilibrium distribution of rod orientations; the director has been oriented at the angle α . (b) The distorted distribution due to shear.

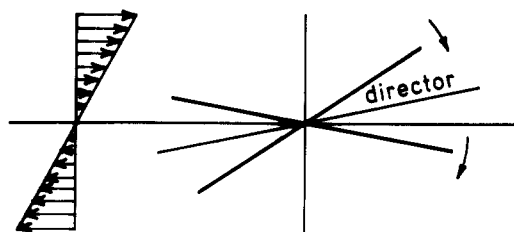


Figure 3. Torque exerted by shear flow on individual rods.

two possible outcomes. In other words, either positive or negative normal stresses can be generated by the same mechanism, depending on conditions. It can perhaps be expected that, by varying those conditions, the system might switch from one situation to the other. It is fair to note that Chaffey and Porter¹¹ had already indicated the conflict between shear and intermolecular potential as the possible source of negative normal stresses in liquid-crystalline polymers.

In the preceding discussion, we have only considered those cases for which a stationary distribution of rod orientations is anyhow achieved. The rest of the paper also deals with this situation only. Of course, a time-independent distribution is not incompatible with the notion that the particles continuously rotate as a consequence of the shear flow. Indeed, for the isotropic phase, this is what occurs at all values of the shear rate. On the other hand, for the nematic phase, the existence of a stationary solution cannot be guaranteed beforehand. The alternative is a tumbling of the whole distribution, not only of the individual rods. In what follows, we find the domain of ex-

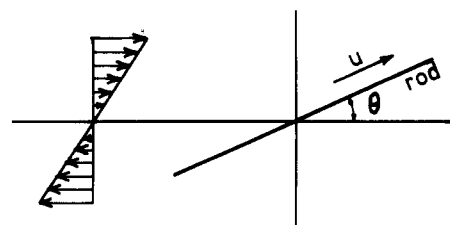


Figure 4. Orientation of a rod determined by the angle θ between the rod axis and the shear direction.

istence of the stationary solution and give results within that range only.

Oriental Distribution in Two Dimensions

We assume that all rods in the system are parallel to a plane and consider shear flow in that plane as in Figure 4. The angle θ or the unit vector $\mathbf{u} \equiv (\cos \theta, \sin \theta)$ is used to specify the orientation of a rod in the plane.

As also done by Doi,⁷ we assume that the nematic state is brought about by a quadratic potential, i.e., of the Maier-Saupe type, having the form

$$V(\mathbf{u}) = -2Uk_B T \langle \mathbf{u} \mathbf{u} \rangle : \mathbf{u} \mathbf{u} \quad (1.1)$$

where $k_B T$ is the Boltzmann constant times the absolute temperature, U is the nondimensional intensity of the potential, and $\langle \rangle$ indicates the average over the existing \mathbf{u} distribution. V as an absolute minimum if all the rods are parallel to one another. Notice also that, in eq 1.1, \mathbf{u} and $-\mathbf{u}$ give rise to the same value of V , as it should be. In terms of the angle θ , eq 1.1 may be written as

$$V(\theta) = -Uk_B T (\langle \cos 2\theta \rangle \cos 2\theta + \langle \sin 2\theta \rangle \sin 2\theta) \quad (1.2)$$

showing explicitly the periodicity of period π .

Taken by itself, the shear flow would make a thin rod rotate with an angular velocity given by

$$\dot{\theta} = -\Gamma \sin^2 \theta \quad (1.3)$$

where Γ is the shear rate. By "thin" we mean a rod with such a large length-to-thickness ratio that the effect of its nonzero thickness can be neglected.

The angular flux of rods is then written as

$$J = -D(\partial f / \partial \theta + f / k_B T \partial V / \partial \theta) - \Gamma f \sin^2 \theta \quad (1.4)$$

where $f(\theta)$ is the orientational distribution function and D is the rotational diffusivity of the rods. Partial derivatives appear in eq 1.4 because in general $f(\theta)$, and consequently $V(\theta)$, will vary with time. In such a case, J will depend on θ as well as on time. In this work, however, we only look for stationary solutions, which then correspond to J being a constant in both time and θ . Thus, if is also D taken to be θ independent,^{7,12} a stationary distribution will obey the equation

$$df/d\theta + P(\theta)f = C \quad (1.5)$$

where C is a constant, and

$$P(\theta) = (1/k_B T) dV/d\theta + (\Gamma/D) \sin^2 \theta \quad (1.6)$$

The general solution of eq 1.5 is then

$$f(\theta) = C \exp\{-g(\theta)\} \left(\int_0^\theta \exp\{g(x)\} dx + K \right) \quad (1.7)$$

In eq 1.7, K is another constant and $g(\theta)$ is an integral function of $P(\theta)$; i.e.,

$$g(\theta) = -U(\langle \cos 2\theta \rangle \cos 2\theta + \langle \sin 2\theta \rangle \sin 2\theta) + G(\theta - (1/2) \sin 2\theta) \quad (1.8)$$

where

$$G = \Gamma/2D \quad (1.9)$$

is a nondimensional shear rate.

We must now require that $f(\theta)$ be properly periodic, i.e., of period π . By letting $f(\pi)$ be equal to $f(0)$, we determine K as

$$K = \frac{\int_0^\pi \exp\{g(x)\} dx}{\exp(\pi G) - 1} \quad (1.10)$$

It can be readily verified that, with this K value, $f(\theta + \pi)$ equals $f(\theta)$ identically. Thus, eq 1.7, with $g(\theta)$ and K given by eq 1.8 and 1.10, respectively, provides the orientational distribution function for our problem. The constant C is obtained through the normalization condition

$$\int_0^\pi f(\theta) d\theta = 1 \quad (1.11)$$

When $G = 0$, i.e., at equilibrium, eq 1.7 becomes

$$f(\theta) = C \exp\{-g_0(\theta)\} \quad (1.12)$$

where

$$g_0(\theta) = V/k_B T = -U(\langle \cos 2\theta \rangle \cos 2\theta + \langle \sin 2\theta \rangle \sin 2\theta) \quad (1.13)$$

That is, $f(\theta)$ reduces to a Boltzmann distribution.

It should be emphasized that the expressions so far obtained for $f(\theta)$ are less simple than they might superficially appear. The presence of the averages $\langle \cos 2\theta \rangle$ and $\langle \sin 2\theta \rangle$ in $g(\theta)$ or $g_0(\theta)$ implies that eq 1.7 or 1.12 does not determine $f(\theta)$ explicitly, since $f(\theta)$ appears again within those averages. Starting with the simpler case of the equilibrium situation, we show in the following a way of dealing with this problem.

Statics of the Two-Dimensional Nematics

Under equilibrium conditions, the orientational distribution is symmetric about the director. Moreover, since the orientation of the director is arbitrary, we may set, say, $\langle \sin 2\theta \rangle = 0$, by orienting the director along the horizontal axis in Figure 4. We then rewrite eq 1.12 as

$$f(\theta) = C \exp(a \cos 2\theta) \quad (2.1)$$

where we have set

$$a = U \langle \cos 2\theta \rangle \quad (2.2)$$

By use of the definition of averages, as well as eq 2.1 and 1.11, eq 2.2 is now written as

$$\frac{a}{U} = \frac{\int_0^\pi \cos 2\theta \exp(a \cos 2\theta) d\theta}{\int_0^\pi \exp(a \cos 2\theta) d\theta} \quad (2.3)$$

For a given U , eq 2.3 must be solved for the unknown a . To this end, it is convenient to integrate by parts the numerator in eq 2.3, thus obtaining

$$\frac{a}{U} = \frac{a \int_0^\pi \sin^2 2\theta \exp(a \cos 2\theta) d\theta}{\int_0^\pi \exp(a \cos 2\theta) d\theta} \quad (2.4)$$

Equation 2.4 shows that, whatever value is given to U , $a = 0$ is a solution of the equation. A single, nonzero, additional solution, called a^* , is found only if $U > 2$. In fact,

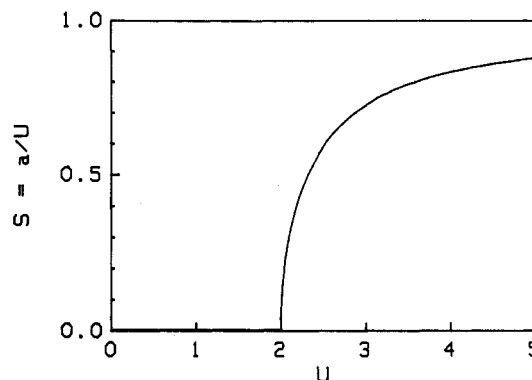


Figure 5. Order parameter as a function of the interaction potential. $U = 2$ marks the isotropic-nematic transition.

after division by a , eq 2.4 defines a monotonically increasing function $U(a) = 1/\langle \sin^2 2\theta \rangle$, the lower limit of which can readily be calculated analytically as $U(0) = 2$. The rest of the function is obtained by evaluating the integrals numerically. The inverse of this function is $a^*(U)$.

Clearly, $a = 0$ corresponds to the isotropic phase, whereas $a = a^*$ to the nematic one. To investigate the stability of these solutions, we consider the free energy A of the system. Since $f(\theta)$ describes the orientational probability and $-U \langle \cos 2\theta \rangle \cos 2\theta$ is the mean-field interaction potential acting on a rod, we write

$$A/c k_B T = \langle \ln f(\theta) \rangle - U/2 \langle \cos 2\theta \rangle^2 \quad (2.5)$$

where c is the number of rods in the system. By use of eq 2.1 and 2.2, as well as the expression for the normalization constant C , eq 2.5 is rewritten as

$$A/c k_B T = a^2/2U - \ln \left[\int_0^\pi \exp(a \cos 2\theta) d\theta \right] \quad (2.6)$$

For a given U , A is to be minimized with respect to a . By setting the a derivative of the previous expression equal to zero, we again find eq 2.3, as we should. By further calculating the second derivative, we find that, at $a = 0$, A is minimum as long as $U < 2$, whereas for $U > 2$ A is maximum at $a = 0$ and minimum at $a = a^*$. Thus, $U = 2$ marks the isotropic-nematic transition.

Notice finally that, in two dimensions, the order parameter has to be defined as

$$S \equiv 2(\langle \cos^2 \theta \rangle - 1/2) \quad (2.7)$$

so as to become zero in the isotropic case and unity in the fully aligned one. Therefore,

$$S = \langle \cos 2\theta \rangle = a/U \quad (2.8)$$

Thus, a^* is all we need to complete the equilibrium calculations. Figure 5 reports the order parameter as a function of U for our two-dimensional nematics.

Stationary Solution in Shear

In order to explicitly determine $f(\theta)$ in the presence of shear, it is expedient to replace the θ variable with the angle ϕ , defined as

$$\theta = \alpha + \phi \quad (3.1)$$

where the angular shift α ($-\pi/4 \leq \alpha \leq \pi/4$) is chosen so as to obtain

$$\langle \sin 2\phi \rangle = 0 \quad (3.2)$$

In a way, one might think of α as being the angular position of the director when shear is present, though, of course, the director becomes ill defined for a distorted, i.e.,

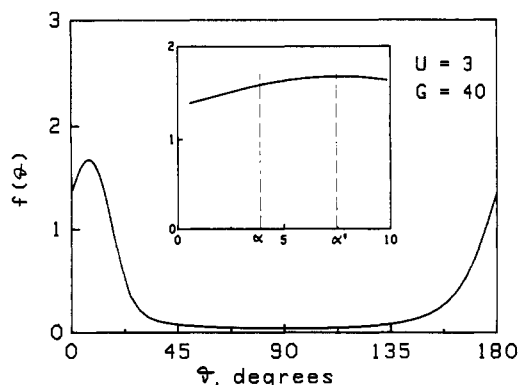


Figure 6. Orientational distribution function, $f(\theta)$, under shear. The inset shows, in an expanded scale, the difference between α and α^* .

no longer symmetric, orientational distribution.

Rephrased in the ϕ variable, the previously found expression of the distribution function becomes

$$f(\phi) = C \exp\{-g(\phi)\} \left(\int_0^\phi \exp[g(x)] dx + K \right) \quad (3.3)$$

$$g(\phi) = -a \cos 2\phi + G\{\phi - (1/2) \sin(2\alpha + 2\phi)\} \quad (3.4)$$

Equations 3.3 and 3.4 replace eq 1.7 and 1.8, whereas eq 1.10 for K remains the same, provided the function g is now interpreted as that given by eq 3.4. Notice that, in writing eq 3.4, we have used the condition of eq 3.2 and that, similarly to the previous section, we have set

$$a = U \langle \cos 2\phi \rangle \quad (3.5)$$

We now write eq 3.2 more explicitly as

$$\int_0^\pi \sin 2\phi \exp\{-g(\phi)\} \left(\int_0^\phi \exp[g(x)] dx + K \right) d\phi = 0 \quad (3.6)$$

and observe that, for a given a value, the only unknown quantity in eq 3.6 is α . Thus, by some appropriate trial-and-error procedure, the value of α can be calculated from eq 3.6. Once α has been determined, the distribution function, including the normalization constant C , is known completely. This allows one to calculate $\langle \cos 2\phi \rangle$ and therefore U from eq 3.5.

Repeating the above procedure for a set of values of a and G , the function $\alpha(U, G)$ is generated. This function, together with the associated dependencies on U and G of all other quantities appearing in eq 3.3 and 3.4 (i.e., a , K , and C), completely solves our problem.

The solution is not always found, however. We find one (and only one) solution throughout the range of G values explored ($0 < G < 10^3$) only for values of U less than ca. 2.41, thus encompassing the whole isotropic range ($0 \leq U \leq 2$), as well as a small segment of the nematic range ($2 < U < 2.41$).

Conversely, for $U > 2.41$, a lower bound for G is found, called G_{critical} , below which the stationary solution disappears. We infer that, for $G < G_{\text{critical}}$, the system switches to the tumbling situation. G_{critical} appears to grow steadily with increasing U .

Figure 6 shows a typical stationary distribution function. Notice that the angular position of the maximum of the distribution, called α^* , does not coincide with α . It is, in fact, significantly larger than α . The difference between α and α^* is a measure of the skewness of the distribution.

Figure 7 shows the dependence of α and α^* on G and U . Quite amazingly, both α and α^* are found to be *negative* in a range of G values just above G_{critical} . Then, by increasing G , α and α^* first grow to positive values, reach

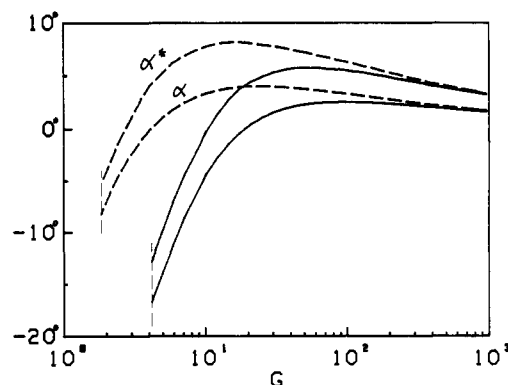


Figure 7. Dependence of α and α^* on G and U . Solid curves refer to $U = 5$, dashed ones to $U = 3$. Notice the negative values just above G_{critical} .

a maximum, and then steadily decrease again, while remaining positive.

As far as the spread of the distribution is concerned, it is found that $\langle \sin^2 2\phi \rangle$ at G_{critical} is much above the equilibrium value, i.e., the distribution is *less peaked* than at equilibrium. Then, with increasing G , $\langle \sin^2 2\phi \rangle$ steadily decreases toward zero, thus eventually passing through the equilibrium value. For $U = 3$ and 5, the crossover takes place at about $G = 7$ and 60, respectively.

As shown by Figure 7, at large G values, the results become asymptotically independent of U . This independence is comprehensible when it is observed that, in the expression for $g(\phi)$ of eq 3.4, the second term becomes dominant, at large G values, with respect to the first, U -dependent one.

The disappearance of the stationary solution, taking place when U becomes larger than ca. 2.41, is seen more directly in the limit of G approaching zero, because the mathematics simplifies considerably in that linear limit. By expanding the previous expressions around $G = 0$, after some manipulations, we find that α is obtained explicitly in this case, i.e., through the equation

$$\cos 2\alpha = (M - 1/M)/N \quad (\text{small } G) \quad (3.7)$$

where

$$M = (1/\pi) \int_0^\pi \exp(a \cos x) dx$$

$$N = (1/\pi) \int_0^\pi \cos x \exp(a \cos x) dx \quad (3.8)$$

The a value in eq 3.8 is the equilibrium value in this limit, i.e., that reported as a/U versus U in Figure 5. Indeed, the whole distribution is the equilibrium distribution. In the nematic phase, the shear flow only affects the orientation of the director by either imposing a value of α or generating the tumbling situation.

As long as $a = 0$ ($U < 2$), the phase is isotropic, and eq 3.7 predicts the classical result; i.e., $\cos 2\alpha = 0$, $\alpha = \pm\pi/4$. In other words, the shear makes the distribution slightly ellipsoidal, with the axes of the ellipse oriented at $\pm\pi/4$. Upon transition to the nematic phase ($U = 2$), the value of a rapidly drops to smaller values and keeps decreasing as U (and therefore a) increases. At $U \approx 2.41$, the solution of eq 3.7 disappears, since the value of $(M - 1/M)/N$ becomes larger than unity. The system is of the tumbling type thereafter.

It may be worth noting that the switch from shear orienting to a tumbling situation, which is observed in some small molecule nematics by changing the temperature,¹³ takes place always in the direction of a decreasing temperature, i.e., when the strength of the nematic potential

is increased. The prediction of the present theory is consistent with this observation.

Elastic Contribution to the Stress Tensor

The free energy of the system may be written as

$$A/c k_B T = \langle \ln f(\mathbf{u}) \rangle - U \langle \mathbf{u} \mathbf{u} \rangle : \langle \mathbf{u} \mathbf{u} \rangle \quad (4.1)$$

where, as in eq 2.5, the first term is due to the orientational entropy and the second to rod interactions.

As also done by Doi and Edwards,¹² we now imagine that a small deformation \mathbf{Q} is instantaneously applied and equate the corresponding change δA of the free energy per unit volume to the work done by the existing stress:

$$\delta A = \mathbf{Q} : \boldsymbol{\sigma}^E \quad (4.2)$$

More precisely, since δA equals the reversible work, eq 4.2 only involves the elastic contribution to the stress tensor, $\boldsymbol{\sigma}^E$. In a later section, the viscous contribution will be accounted for.

Now, upon applying \mathbf{Q} , \mathbf{u} goes to \mathbf{u}' given by

$$\mathbf{u}' = \mathbf{u} + \mathbf{Q} \cdot \mathbf{u} - (\mathbf{Q} : \mathbf{u} \mathbf{u}) \mathbf{u} \quad (4.3)$$

At the same time, conservation of the rods contained in the interval \mathbf{u} to $\mathbf{u} + d\mathbf{u}$ (i.e., between θ and $\theta + d\theta$) requires that

$$f'(\mathbf{u}') d\mathbf{u}' = f(\mathbf{u}) d\mathbf{u} \quad (4.4)$$

from which the following relationship can be obtained:

$$f'(\mathbf{u}') = f(\mathbf{u}) (1 + 2\mathbf{Q} : \mathbf{u} \mathbf{u}) \quad (4.5)$$

Then, by keeping only first-order terms in \mathbf{Q} , we calculate δA as

$$\delta A / c k_B T = 2\mathbf{Q} : \{ \langle \mathbf{u} \mathbf{u} \rangle - 2U \langle \langle \mathbf{u} \mathbf{u} \rangle \cdot \langle \mathbf{u} \mathbf{u} \rangle - \langle \mathbf{u} \mathbf{u} \mathbf{u} \mathbf{u} \rangle : \langle \mathbf{u} \mathbf{u} \rangle \} \quad (4.6)$$

Comparison of eq 4.2 and 4.6 shows that

$$\boldsymbol{\sigma}^E / 2c k_B T = (1 - 2U) \langle \mathbf{u} \mathbf{u} \rangle + 2U \langle \mathbf{u} \mathbf{u} \mathbf{u} \mathbf{u} \rangle : \langle \mathbf{u} \mathbf{u} \rangle \quad (4.7)$$

In writing eq 4.7, we have used the fact that, in two dimensions, $\langle \mathbf{u} \mathbf{u} \rangle \cdot \langle \mathbf{u} \mathbf{u} \rangle$ differs from $\langle \mathbf{u} \mathbf{u} \rangle$ only by an irrelevant isotropic term.

The component form of eq 4.7 reads

$$\begin{aligned} \sigma_{12}^E / c k_B T &= \langle \sin 2\theta \rangle + U \langle \cos 2\theta \rangle \langle \sin 4\theta \rangle / 2 - \\ &\langle \sin 2\theta \rangle \langle \cos^2 2\theta \rangle (\sigma_{11}^E - \sigma_{22}^E) / 2c k_B T = \langle \cos 2\theta \rangle + \\ &U \langle \sin 2\theta \rangle \langle \sin 4\theta \rangle / 2 - \langle \cos 2\theta \rangle \langle \sin^2 2\theta \rangle \end{aligned} \quad (4.8)$$

It can readily be verified that these expressions properly go to zero at equilibrium. Indeed, by orienting the director so that, say, $\langle \sin 2\theta \rangle = 0$, then it follows that $\langle \sin 4\theta \rangle = 0$ and $\langle \sin^2 2\theta \rangle = 1/U$ (see eq 2.4).

For the case of shear flow, it may be convenient to use the equivalent expressions in terms of ϕ and α . Equations 4.8 then become

$$\begin{aligned} \sigma_{12}^E / c k_B T &= \langle \cos 2\phi \rangle \{ \sin 2\alpha (1 - \\ &U \langle \sin^2 2\phi \rangle) + (U/2) \cos 2\alpha \langle \sin 4\phi \rangle \} \\ (\sigma_{11}^E - \sigma_{22}^E) / c k_B T &= 2 \langle \cos 2\phi \rangle \{ \cos 2\alpha (1 - \\ &U \langle \sin^2 2\phi \rangle) - (U/2) \sin 2\alpha \langle \sin 4\phi \rangle \} \end{aligned} \quad (4.9)$$

By use of the results described in the previous section, all quantities appearing in these equations are readily calculated. Figure 8 shows a sample of the results that are obtained for values of U above 2.41. Needless to say, the elastic stress plotted in Figure 8 could be obtained only for $G > G_{\text{critical}}$.

Figure 8 shows that the normal stress difference is negative for a range of G values above G_{critical} . This feature

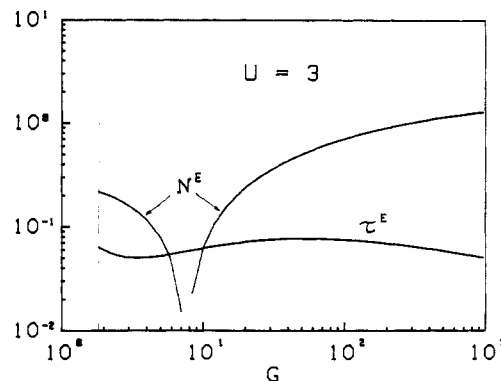


Figure 8. Elastic stress for a value of U larger than 2.41. $N^E = (\sigma_{11}^E - \sigma_{22}^E) / c k_B T$ is negative to the left and positive to the right. $\tau^E = \sigma_{12}^E / c k_B T$ does not always increase with increasing G .

is found for all values of U , as long as $U > 2.41$, the negative-to-positive transition being displaced to larger G values as U increases. It should be noted that the range of negative normal stresses extends well beyond the range of negative values of α and α^* (see Figure 7). Rather, the value of G at which the normal stresses change sign essentially coincides with that at which $\langle \sin^2 2\phi \rangle$ crosses the equilibrium value $1/U$. This confirms that the negative normal stress effect is due to an increased spread of rod orientations with respect to equilibrium rather than to any anomalous orientation of the director.

The elastic shear stress, also shown in Figure 8, is found to be always positive. A possibly disturbing feature is nevertheless apparent in Figure 8, i.e., in some ranges of G values the shear stress decreases with increasing G , which might imply that the flow is not stable. We still miss a term, however, which is the viscous contribution to the total stress. Thus, further discussion of these results, as well as of those for $U < 2.41$, is postponed to the following section, where that contribution is calculated.

Viscous Contribution and Total Stress

For rodlike polymers, the viscous stress is linked to the velocity gradient \mathbf{L} , through the equation (compare eq 8.121 of ref 14)

$$\boldsymbol{\sigma}^V = c \zeta \mathbf{L} : \langle \mathbf{u} \mathbf{u} \mathbf{u} \mathbf{u} \rangle \quad (5.1)$$

where ζ is a suitable friction coefficient.

For shear flow, eq 5.1 becomes

$$\sigma^V = c \zeta \Gamma \langle u_1 u_2 \mathbf{u} \mathbf{u} \rangle \quad (5.2)$$

where, of course, $u_1 = \cos \theta$ and $u_2 = \sin \theta$. In nondimensional form, eq 5.2 is rewritten as

$$\sigma^V / c k_B T = \beta G \langle u_1 u_2 \mathbf{u} \mathbf{u} \rangle \quad (5.3)$$

where G is given by eq 1.9 and β represents, within a numerical coefficient of order unity, the ratio of two friction coefficients or, equivalently, of two diffusivities:

$$\beta \approx D / D_0 \quad (5.4)$$

In eq 5.4, D is the same diffusivity as that appearing in eq 1.4, i.e., the rotational diffusivity in the actual system, which is a concentrated solution of rods. Conversely, D_0 is the rotational diffusivity of the rods in a dilute solution, since the friction coefficient appearing in eq 5.1 merely describes the rod-solvent frictional interaction. Because of the rotational hindrances exerted on a rod by the surrounding ones in a concentrated solution, D is expected to be smaller, possibly much smaller, than D_0 .¹²

Unfortunately, the value of β is, as yet, not well determined from either theory or experiment.^{14,15} Thus, we have to consider β as an adjustable parameter, with the only

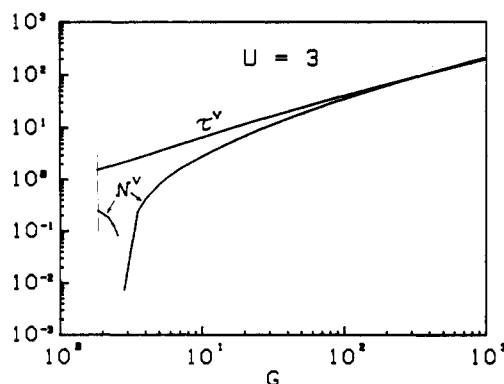


Figure 9. Viscous stress for $U = 3$. $N^v = (\sigma_{11}^v - \sigma_{22}^v)/\beta ck_B T$; $\tau^v = \sigma_{12}^v/\beta ck_B T$.

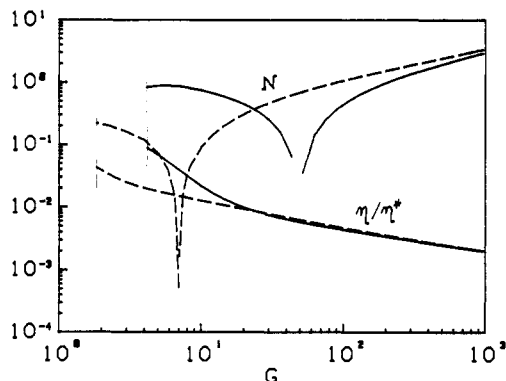


Figure 10. Typical viscosity and normal stress results for U larger than 2.41. Solid curves refer to $U = 5$, dashed ones to $U = 3$. In summing σ^v to σ^E , $\beta = 10^{-2}$ has been used.

restriction being that it must be smaller, possibly much smaller, than unity.

In component form, eq 5.3 becomes

$$\begin{aligned}\sigma_{12}^v/ck_B T &= \beta G(1 - \langle \cos 4\theta \rangle) \\ (\sigma_{11}^v - \sigma_{22}^v)/ck_B T &= 2\beta G\langle \sin 4\theta \rangle\end{aligned}\quad (5.5)$$

in which an additional numerical factor of 1/8 has been incorporated in the unknown value of β . In terms of α and ϕ , eq 5.5 obviously become

$$\begin{aligned}\sigma_{12}^v/ck_B T &= \beta G(1 - \cos 4\alpha\langle \cos 4\phi \rangle + \sin 4\alpha\langle \sin 4\phi \rangle) \\ (\sigma_{11}^v - \sigma_{22}^v)/ck_B T &= 2\beta G(\sin 4\alpha\langle \cos 4\phi \rangle + \cos 4\alpha\langle \sin 4\phi \rangle)\end{aligned}\quad (5.6)$$

Figure 9 shows the typical behavior of the viscous stress as a function of G . Notice that even the viscous contribution to the normal stress difference is negative for G close to G_{critical} , due to the negative α values. The shear stress, on the other hand, is always positive and grows steadily with increasing G .

Before combining results such as those of Figures 8 and 9, a decision about β must be made. When the distribution becomes more peaked, the hindrances to rotation of the rods decrease and D increases.^{7,14} Hence, β is expected to increase with increasing Γ . For the sake of simplicity, however, we have chosen a constant value of β ($\beta = 1/100$) to produce the curves reported in Figure 10. Instead of the shear stress, we have reported the viscosity, in non-dimensional form, given by

$$\eta/\eta^* = \sigma_{12}/Gck_B T = (\sigma_{12}/\Gamma)/(ck_B T/2D) \quad (5.7)$$

It can be shown that $\eta^* = ck_B T/2D$ has the meaning of 4 times the zero-shear viscosity which would be found in the isotropic solution were the value of the rotational diffusivity the same as in the nematic phase.

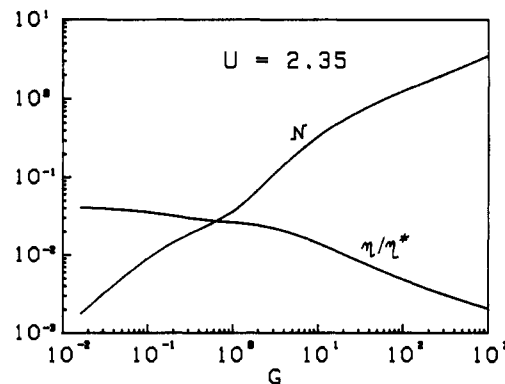


Figure 11. One result in the range $2 < U < 2.41$. The normal stress difference is found to be always positive in this case.

Figure 10 shows that adding the viscous contribution makes the flow stable (the negative slope of the viscosity curve is less than 1) at large G values. With the value of β we have chosen, there remains a zone of instability close to G_{critical} . For a somewhat larger value of β ($\beta = 0.1$, say), that instability would also disappear. The normal stress difference remains negative in a wide range of G values in any event. In fact, the shape of the curves which are produced is remarkably similar to what is found experimentally at large values of the shear rate.³⁻⁶ When comparing these predictions with experiments performed at different concentrations, i.e., at different U values, it should be remembered that the dimensionless shear rate (G) also depends on concentration through the diffusivity (D).

Figure 11 reports the results obtained in the range $2 < U < 2.41$. These should be compared with experiments made at concentrations just above the isotropic-nematic transition. Comparison with the data in Figure 11 of ref 3 shows again a very good qualitative agreement. In particular, the bump in the normal stress curve is faithfully reproduced. In view of the two-dimensional character of the present analysis, a word of caution is nevertheless required. In particular, we recall that the linear theory in three dimensions¹⁰ does not predict a nontumbling U range, however small, just above the isotropic-nematic transition. On the other hand, the region close to the transition is prone to be particularly sensitive not only to dimensionality but also to the form of the potential. The form chosen here, as well as in ref 10, is the simplest plausible one. It cannot be excluded that more realistic potentials might produce, in three dimensions as well, a behavior similar to that found here. Indeed, we believe that what essentially determines the choice between tumbling and nontumbling in the linear range is the spread of the distribution, i.e., the equilibrium value of the order parameter S . Experimental values of S close to the transition are typically below those predicted by the three-dimensional theory based on the potential of eq 1.1.

Finally, Figure 12 collects viscosity results for a range of U values that also includes the isotropic phase ($U \leq 2$). Consistently with the definition of η^* , the zero-shear value of η/η^* is found to be 0.25 for $U \leq 2$. It may be observed that one effect of the nematic potential in the isotropic phase is that of enhancing the non-Newtonian character of the viscosity. Indeed, separation of the viscosity curve from the Newtonian zero-shear plateau occurs at smaller G values for $U = 2$ than for $U = 1$.

At large G values, we expect that D becomes equal to D_0 and is, therefore, independent of concentration. Thus, since Figure 12 shows that all curves of η/η^* become coincident at large G values, we may deduce that, for a

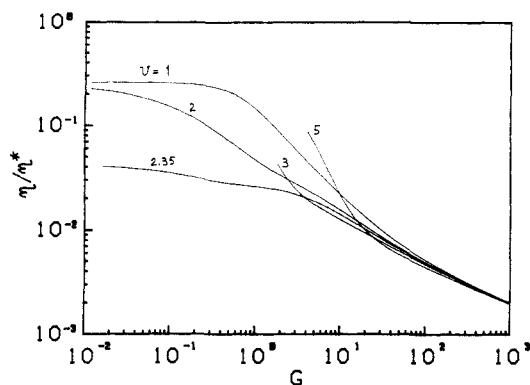


Figure 12. Viscosity curves for both the isotropic and the nematic phases.

given Γ , η is proportional to c in that region (see eq 5.7). Also this prediction compares favorably with data such as those reported in Figure 3 of ref 3.

Concluding Remarks

We can summarize the predictions of the model developed in this work in the following way.

Insofar as tumbling is concerned, two distinct effects emerge from the analysis. One of them is linked to the orientational spread at equilibrium. As long as the equilibrium distribution is not too peaked, there is no tumbling. This obviously applies to the isotropic phase, but it goes over to the nematic one, provided the nematic potential is not too intense.

When U increases and therefore the equilibrium distribution becomes considerably peaked, tumbling appears. However, with increasing G , it again disappears, possibly because of the fast rotation of the individual rods, which takes place as soon as they have passed the $\Theta = 0$ orientation and which brings them back (after a turn of approximately π) to rejoin the majority of the other rods, lingering, so to speak, in the neighborhood of $\Theta = \alpha$. The mechanism is the same as in the isotropic phase; in fact, all results become similar at large G values, i.e., when the influence of U is comparatively negligible.

The negative normal stress effect, though present in the viscous contribution as well, is mostly an elastic effect, to be associated with an increase in the orientational spread with respect to equilibrium. The increase in spread is brought about by the rotational quality of a shear field. Comparison of the predictions of this theory with the experimental results indicates that the effect already starts in the tumbling region and survives for a while in the G range above G_{critical} , where stationary solutions are found.

In view of the good qualitative agreement with the experimental results, we are inclined to believe that the two-dimensional analysis has caught the essential actual

behavior, i.e., that the mechanisms discussed here remain essentially the same in three dimensions as well. Of course, differences are also to be expected. One prominent difference is already apparent in the equilibrium results. In two dimensions, the isotropic-nematic transition becomes a second-order transition, as shown by the order parameter behavior depicted in Figure 5. The same figure shows, however, that the order parameter, though continuous at the transition, rises steeply after it. Therefore, albeit conceptually important, this difference might be virtually irrelevant in practice.

In comparing theoretical predictions with experiments, another important difference to keep in mind is the fact that liquid-crystalline polymers are not really rodlike. In most cases, they incorporate various elements of flexibility in the chain. How to account for partial rigidity, for flexible spacers, etc., in rheological theory, is not clear at the moment.

A last remark concerns the numerical calculations made in this work. Although conceptually very simple, the integrations require some care in dealing with (i) highly peaked distribution functions and (ii) large values of $g(x)$ in the positive and negative exponentials simultaneously appearing in equations like eq 3.3. It should also be mentioned that some uncertainty exists in the values of G_{critical} , in the sense that their true values might be somewhat smaller than reported here. Indeed, since the solutions of eq 3.6 are determined by a trial-and-error procedure (a Newton-Raphson scheme), failure to find a solution does not necessarily imply that the solution does not exist. Details about these aspects can be obtained from one of the authors (P.L.M.).

Acknowledgment. This work was supported by Ministero Pubblica Istruzione, Rome.

References and Notes

- (1) Onsager, L. *Ann. N. Y. Acad. Sci.* **1949**, *51*, 627.
- (2) Flory, P. J. *Proc. R. Soc. London* **1956**, *A234*, 73.
- (3) Kiss, G.; Porter, R. S. *J. Polym. Sci., Polym. Symp.* **1978**, *No. 65*, 193.
- (4) Kiss, G.; Porter, R. S. *J. Polym. Sci., Polym. Phys. Ed.* **1980**, *18*, 361.
- (5) Navard, P. *J. Polym. Sci., Polym. Phys. Ed.* **1986**, *24*, 435.
- (6) Berry, G. C. *Mol. Cryst. Liq. Cryst.* **1988**, *165*, 333.
- (7) Doi, M. *J. Polym. Sci., Polym. Phys. Ed.* **1981**, *19*, 229.
- (8) Marrucci, G. *Mol. Cryst. Liq. Cryst.* **1982**, *72L*, 153.
- (9) Semenov, A. N. *Zh. Eksp. Teor. Fiz.* **1983**, *85*, 549.
- (10) Kuzuu, N.; Doi, M. *J. Phys. Soc. Jpn.* **1983**, *52*, 3486; **1984**, *53*, 1031.
- (11) Chaffey, C. E.; Porter, R. S. *J. Rheol. (N. Y.)* **1985**, *29*, 281.
- (12) Doi, M.; Edwards, S. F. *J. Chem. Soc., Faraday Trans. 2* **1978**, *74*, 560; **1978**, *74*, 918.
- (13) Pieranski, P.; Guyon, E. *Commun. Phys.* **1976**, *1*, 45.
- (14) Doi, M.; Edwards, S. F. *The Theory of Polymer Dynamics*; Clarendon Press: Oxford, 1986.
- (15) Doi, M.; Yamamoto, I.; Kano, F. *J. Phys. Soc. Jpn.* **1984**, *53*, 3000.